

# First e-VLBI observations of Cygnus X-3

V. Tudose,<sup>1,2\*</sup> R. P. Fender,<sup>1,3</sup> M. A. Garrett,<sup>4</sup> J. C. A. Miller-Jones,<sup>1</sup> Z. Paragi,<sup>4</sup>  
R. E. Spencer,<sup>5</sup> G. G. Pooley,<sup>6</sup> M. van der Klis<sup>1</sup> and A. Szomoru<sup>4</sup>

<sup>1</sup>*Astronomical Institute 'Anton Pannekoek', University of Amsterdam, Kruislaan 403, 1098 SJ Amsterdam, the Netherlands*

<sup>2</sup>*Astronomical Institute of the Romanian Academy, Cutitul de Argint 5, RO-040557 Bucharest, Romania*

<sup>3</sup>*School of Physics and Astronomy, University of Southampton, Highfield, Southampton SO17 1BJ*

<sup>4</sup>*Joint Institute for VLBI in Europe, Postbus 2, 7990 AA Dwingeloo, the Netherlands*

<sup>5</sup>*University of Manchester, Jodrell Bank Observatory, Macclesfield, Cheshire SK11 9DL*

<sup>6</sup>*University of Cambridge, Mullard Radio Astronomy Observatory, J. J. Thomson Avenue, Cambridge CB3 0HE*

Accepted 2006 November 2. Received 2006 November 2; in original form 2006 October 26

## ABSTRACT

We report the results of the first two 5-GHz electronic very-long-baseline interferometry (e-VLBI) observations of the X-ray binary Cygnus X-3 using the European VLBI Network. Two successful observing sessions were held, on 2006 April 20, when the system was in a quasi-quiet state several weeks after a major flare, and on 2006 May 18, a few days after another flare. At the first epoch we detected faint emission probably associated with a fading jet, spatially separated from the X-ray binary. The second epoch in contrast reveals a bright, curved, relativistic jet more than 40 milliarcsec in extent. In the first and probably also second epochs the X-ray binary core is not detected, which may indicate a temporary suppression of jet production as seen in some black hole X-ray binaries in certain X-ray states. Spatially resolved polarization maps at the second epoch provide evidence of interaction between the ejecta and the surrounding medium. These results clearly demonstrate the importance of rapid analysis of long-baseline observations of transients, such as facilitated by e-VLBI.

**Key words:** techniques: interferometric – accretion, accretion discs – radiation mechanisms: non-thermal – stars: individual: Cygnus X-3 – ISM: jets and outflows.

## 1 INTRODUCTION

The X-ray binary Cygnus X-3 was first detected in X-rays by Giacconi et al. (1967). The infrared (e.g. Becklin et al. 1973) and X-ray fluxes (e.g. Parsignault et al. 1972) show a periodicity of 4.8 h which is interpreted as the orbital period of the system. The nature of the compact object is not known (Schmutz, Geballe & Schild 1996; Mitra 1998). As for the companion star, there is compelling evidence pointing toward a WN Wolf-Rayet star (van Kerkwijk et al. 1996; Fender, Hanson & Pooley 1999a; Koch-Miramond et al. 2002).

Giant outbursts and large flares have been observed at radio wavelengths in Cygnus X-3 since 1972 (Gregory et al. 1972). In quiescence the soft X-ray emission is correlated with the radio emission, while the hard X-ray is anti-correlated with the radio; in a flare state, the situation is reversed: the hard X-ray correlates with the radio and the soft X-ray emission is anti-correlated (Watanabe et al. 1994; McCollough et al. 1999; Choudhury et al. 2002).

Radio observations made during such large flares at different resolutions with the Very Large Array (VLA), the Multi-Element Radio Linked Interferometer Network (MERLIN), the Very Long Baseline

Array (VLBA) and the European VLBI Network (EVN) (Geldzahler et al. 1983; Spencer et al. 1986; Molnar, Reid & Grindlay 1988; Schalinski et al. 1995, 1998; Mioduszewski et al. 2001; Martí, Paredes & Peracaula 2001; Miller-Jones et al. 2004) directly show or are consistent with two-sided relativistic jets [with the notable exception of the VLBA observations of a flare in 1997 February, when the jet was apparently one-sided (Mioduszewski et al. 2001)].

## 2 OBSERVATIONS

One of the aims of electronic very-long-baseline interferometry (e-VLBI) is to enable mapping with long-baseline networks of radio telescopes in a manner which makes it possible to map transient phenomena, such as microquasars, in near-real-time. This will provide the ability to make informed decisions about the optimum observing strategy to employ (frequency of observations, array composition, calibrator selection, etc.) and the need for repeated mapping observations, as well as greatly simplifying the observing procedure and improving its reliability. In the case of the EVN, the data are transported to the correlator at the Joint Institute for VLBI in Europe (JIVE) in real-time using IP routed networks, connecting the radio telescopes through national research networks and the pan-European research network GÉANT 2 via the Dutch national

\*E-mail: vtudose@science.uva.nl

research network SURFnet to JIVE. At the time of our observations, a sustainable data rate of  $128 \text{ Mbit s}^{-1}$  could be achieved. This is expected to improve significantly in the near future. A description of some of the development work in this field was given by Parsley et al. (2003) and Szomoru et al. (2004), and reports of more recent development are in preparation (Szomoru et al., in preparation; Strong et al., in preparation). The data are transferred using Mark5A recorders with  $1 \text{ Gbit s}^{-1}$  network interface cards (Whitney 2003).

We observed Cygnus X-3 at 5 GHz on three occasions, on 2006 March 16, April 20 and May 18, using the six antennas forming the current European e-VLBI Network (e-EVN): Onsala 20 m, Torun, Jodrell Bank MkII, Cambridge, Medicina and Westerbork (phased array). The observing run on March 16 was made in response to the first open call for e-EVN observations 2 weeks earlier. Unfortunately, because of technical problems with the off-line correlator software, the data from March 16 were not useable and have been omitted from the present study. In our second e-VLBI session, on April 20, we observed Cygnus X-3 for an effective integration time of about 7 h in a complex experiment consisting of interleaved observations of Cygnus X-3 and GRS 1915+105 [see Rushton et al. (2007) for the latter target]. Occasionally, delay and rate jumps were introduced in the data at the correlator station units, caused by a combination of limited memory buffer size and long correlation jobs. Although the effect was station-based and thus the closure phases were unaffected, this may have resulted in erroneous phase transfer in a couple of phase-referencing scans. The problem was eventually solved by self-calibrating the target data. During this run, the target was in a ‘quiescent’ state, with the flux density levels in the decay phase following the major radio flares in 2006 March. At the beginning of May, Cygnus X-3 underwent another significant flare and we observed it during an active state via a target-of-opportunity proposal for around 12 h on May 18 (Fig. 1). During both observations the amplitude of the flux density variations was around 10 per cent, except for some  $\sim 1$  h long larger enhancements in the flux density registered at the beginning and end of the April run and at the beginning of the May run. Although this might have introduced artefacts in the radio images, we are confident that they would not be of significant importance.

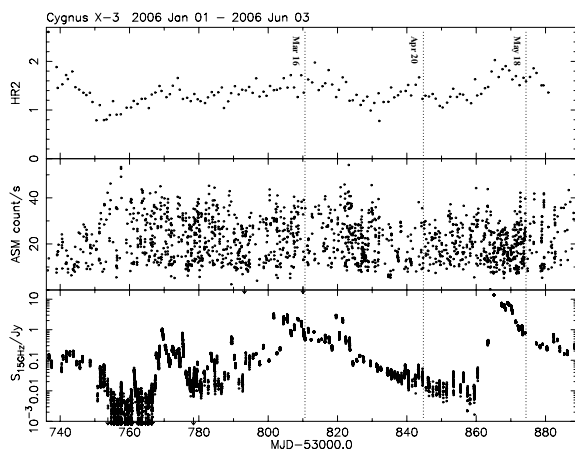


**Figure 1.** Top: *RXTE*/ASM hardness ratio  $HR2 = 5\text{--}12/3\text{--}5$  keV. Middle: *RXTE*/ASM 2–10 keV X-ray light curve. Bottom: 15-GHz radio (Ryle Telescope) light curve. Vertical lines indicate the dates of our e-VLBI observations.

The data were calibrated in AIPS (e.g. Diamond 1995) using standard procedures. For phase referencing we used J2007+4029, a bright ( $\sim 2$  Jy correlated flux) calibrator located  $4.7^\circ$  away from the target, employing a cycle time of 8 min (5 min on the target, 3 min on the phase calibrator). The solutions derived from J2007+4029 were smoothed, extrapolated and applied to Cygnus X-3. The a priori amplitude calibration was improved using the unresolved calibrator J2002+4725. Bandpass calibration was employed, using J2007+4029 in epoch I (2006 April) and J2002+4725 in epoch II (2006 May). We used J2007+4029 as fringe finder in the former run and OQ 208 in the latter. The data were self-calibrated once in phase with a 30-s solution interval and once in amplitude and phase simultaneously with a 30-min solution interval. The resulting radio maps are presented in Fig. 2.

The instrumental polarization leakage (the D-terms) was also determined for epoch II from observations of the unpolarized calibrator OQ 208. For calibration of the electric vector position angles (EVPAs) at VLBI scales we analysed separately the J2007+4029 Westerbork Synthesis Radio Telescope (WSRT) data. We found that this calibrator has a fairly compact polarization structure at VLBI scales enabling us to calibrate the EVPAs with an estimated error of  $10^\circ$ . The distribution of the EVPAs (in the observer frame) and the fractional linear polarization of Cygnus X-3 are shown in Fig. 3. The level of Faraday rotation due to the Galactic interstellar medium, affecting the overall distribution of EVPAs, is unknown and therefore unaccounted for. For an arbitrary high rotation measure in the Galactic plane (Simard-Normandin, Kronberg & Button 1981) of, say,  $200 \text{ rad m}^{-2}$ , the corresponding rotation of the EVPAs at 5 GHz would be up to  $\sim 40^\circ$ .

### 3 RESULTS AND DISCUSSION

Fig. 2 presents the images from 2006 April 20 (epoch I) and May 18 (epoch II). Epoch I reveals a single faint component, possibly slightly resolved, while epoch II reveals a bright curved structure based around three bright knots. Also indicated on Fig. 2 is the location of the X-ray binary radio core as estimated by Miller-Jones et al. (2004; consistent also with Mioduszewski et al. 2001).

In order to facilitate comparison between these two epochs, and more generally to allow us to extract as much information as possible from the observations, we fitted the data in the  $uv$ -plane with elliptical Gaussians using DIFMAP (Shepherd 1997). For epoch I we used one Gaussian while for epoch II we used as a starting model three Gaussians at the positions of the bright features as seen in the radio image before self-calibration. The results are summarized in Table 1. The errors in the coordinates consist of the errors in the position of the calibrator J2007+4029 ( $\sigma_\alpha = 0.000180 \text{ s}$ ;  $\sigma_\delta = 0.00240 \text{ arcsec}$ ; Fey et al. 2004) plus the error in the phase-referencing procedure itself (estimated as  $0.3 \text{ mas}$ ; Pradel, Charlot & Lestrade 2006). We note that owing to the poor  $uv$ -coverage at short baselines the fitted models are not well constrained – in particular the sizes of the Gaussians reported are probably slightly underestimated. Scatter-broadening is an issue for Cygnus X-3; its geometric mean size is  $15 \pm 6 \text{ mas}$  at 5 GHz (Wilkinson, Narayan & Spencer 1994; Schalinski et al. 1995) and might be correlated with the flux at short VLBA baselines (Newell, Garrett & Spencer 1998).

We draw attention to the fact that the maps shown in Fig. 2 account for a small fraction of the total flux density of the source. The 5-GHz e-VLBI integrated flux density measured in the image plane for epoch I is  $4.8 \text{ mJy}$ . However, in the  $uv$ -plane, the data were fitted well by a (larger) elliptical Gaussian with a flux density of  $87 \text{ mJy}$ .

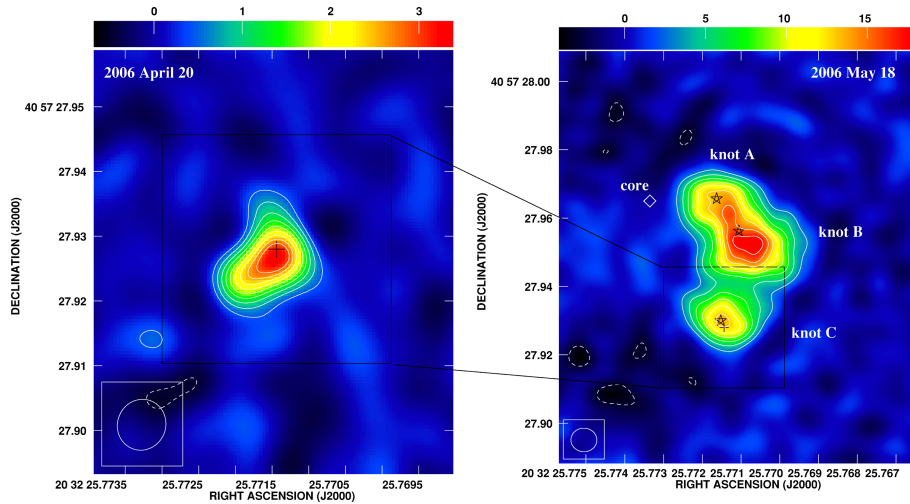


**Figure 2.** Left: 5-GHz *e*-VLBI radio map of Cygnus X-3 on 2006 April 20 (epoch I). The contours are at  $-15, 15, 25, 35, 45, 55, 65, 75, 85$  and  $95$  times the rms noise of  $0.03 \text{ mJy beam}^{-1}$ . The beamsize is  $7.9 \times 7.4 \text{ mas}^2$  at  $\text{PA} = -19^\circ.6$ . The colour code bar on top of the map is expressed in  $\text{mJy beam}^{-1}$ . Right: 5-GHz *e*-VLBI radio map of Cygnus X-3 on 2006 May 18 (epoch II). The contours are at  $-15, 15, 25, 35, 45, 55, 65, 75, 85$  and  $95$  times the rms noise of  $0.2 \text{ mJy beam}^{-1}$ . The beamsize is  $7.6 \times 6.9 \text{ mas}^2$  at  $\text{PA} = 88^\circ.3$ . The colour code bar on top of the map is expressed in  $\text{mJy beam}^{-1}$ . The positions of the centres of the elliptical Gaussians fitted to the data are represented by a cross for epoch I and stars for epoch II. The estimated location of the radio core from Miller-Jones et al. (2004) (J2000 coordinates: RA  $20^{\text{h}}32^{\text{m}}25^{\text{s}}.773\ 35$ , Dec.  $40^\circ57'27''.9650$ ) is indicated with a diamond. Note the change in scale between the two images.

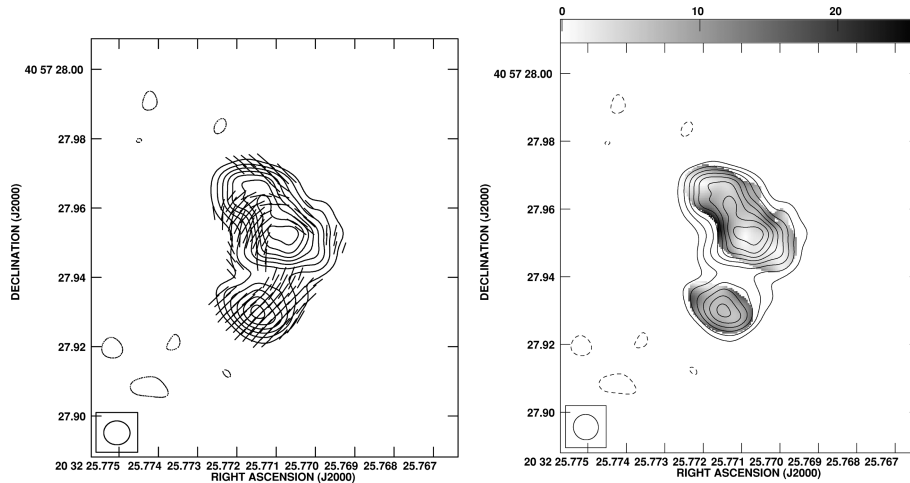


**Figure 3.** 5-GHz *e*-VLBI radio map of Cygnus X-3 on 2006 May 18 (epoch II) with the distribution of the EVPAs (left) and of the fractional linear polarization (right), i.e. the ratio between the polarized flux and the total  $I$  flux,  $(Q^2 + U^2)^{1/2} I^{-1}$  with  $I, Q$  and  $U$  being the Stokes parameters. The code bar is expressed in per cent. In both images the Stokes  $I$  contours are at  $-15, 15, 25, 35, 45, 55, 65, 75, 85$  and  $95$  times the rms noise of  $0.2 \text{ mJy beam}^{-1}$ .

**Table 1.** Results of the  $uv$ -plane elliptical Gaussian fitting. The formal errors in the coordinates (see text) are  $0.000\ 200 \text{ s}$  in RA and  $0.002\ 70 \text{ arcsec}$  in Dec.

| Epoch                   | Component | RA (J2000)   | Dec. (J2000)               | Size<br>(mas $\times$ mas)         | PA<br>( $^\circ$ ) | Flux density<br>(mJy) |
|-------------------------|-----------|--|----------------------------|------------------------------------|--------------------|-----------------------|
| Epoch I – 2006 April 20 | single    | $20^{\text{h}}32^{\text{m}}25^{\text{s}}.771\ 437$ | $+40^\circ57'27''.928\ 00$ | $17.5 \pm 0.3 \times 8.8 \pm 0.5$  | $150 \pm 2$        | $87 \pm 9$            |
| Epoch II – 2006 May 18  | A         | $20^{\text{h}}32^{\text{m}}25^{\text{s}}.771\ 628$ | $+40^\circ57'27''.965\ 66$ | $23.2 \pm 0.7 \times 10.6 \pm 2.5$ | $69 \pm 13$        | $60 \pm 6$            |
|                         | B         | $20^{\text{h}}32^{\text{m}}25^{\text{s}}.771\ 051$ | $+40^\circ57'27''.956\ 21$ | $38.4 \pm 2.1 \times 30.7 \pm 8.1$ | $82 \pm 22$        | $748 \pm 17$          |
|                         | C         | $20^{\text{h}}32^{\text{m}}25^{\text{s}}.771\ 525$ | $+40^\circ57'27''.930\ 00$ | $19.4 \pm 1.1 \times 12.2 \pm 2.3$ | $55 \pm 7$         | $101 \pm 3$           |

For epoch II, the total flux density in the  $uv$ -plane (determined by adding the flux densities contributed by the three elliptical Gaussians fitted to the data) is  $909 \text{ mJy}$  (much of the flux being observed on the shortest baseline), while in the image plane only  $200 \text{ mJy}$

is recovered. The explanation for these differences resides in the fact that because of the lack of  $uv$ -coverage at short baselines the large-scale emission could not be imaged properly. It is also worth mentioning that the simultaneous Westerbork integrated flux density

in epoch II is 1.5 Jy, so at the e-VLBI scale we are missing almost 40 per cent of the emission owing to the unavailability of very short baselines. As an overall comment, the relatively sparse sampling at intermediate baselines has resulted in some considerable loss of flux and uncertainty as to the true strengths of individual knots. While we are confident that the morphology of the imaged structure is real, it is clear that there is a significant, more diffuse component present which we were unable to image.

The single radio-emitting component from epoch I and knot C from epoch II are positionally coincident within uncertainties. This identification of the radio-emitting regions in quiescence and outburst might intuitively lead to the conclusion that the core was located here. However, the large positional discrepancy with the previously estimated core position, plus the high degree of linear polarization (10 per cent, Fig. 3) in the region, suggests that knot C is probably not the core (see further discussion below). Therefore epoch I probably shows not the core but extended radio emission physically separate from the X-ray binary which may be associated with the 2006 March flaring events (Fig. 1). This in turn implies that the core itself was below detection levels, with a  $3\sigma$  upper limit of 0.4 mJy, about two orders of magnitude fainter than typical levels for the source, and four orders of magnitude fainter than the brightest flares. Such ‘quenched’ emission, lasting for periods of weeks to months, was reported before other major flares of Cygnus X-3 (Waltman et al. 1994, 1995; Fender et al. 1997).

Epoch II reveals a much brighter and more complex structure, with the appearance of a curved jet with three bright knots. Knot A is clearly much closer to the previously estimated core location, but is still  $\sim 24$  mas away. Mioduszewski et al. (2001) and Miller-Jones et al. (2004) report the same core position to within 1 mas in data separated by 4.5 yr (but note that this is rather uncertain given the fact that Mioduszewski et al. reported that their phase referencing was not entirely successful). For a distance to Cygnus X-3 of  $\sim 9$  kpc (Predehl et al. 2000) and an arbitrary speed in the plane of the sky of  $100 \text{ km s}^{-1}$ , the upper limit to the positional shift due to the proper motion in the time interval between the observations of Miller-Jones et al. and ours is  $\sim 10.5$  mas. Higher speeds are definitely possible [for instance GRS 1915+105 at  $\sim 11$  kpc has a proper motion of  $\sim 5.8 \text{ mas yr}^{-1}$  (Dhawan, Mirabel & Rodríguez 2000)], but given the present knowledge we cannot confidently identify the proper motion of the system as the cause of the shift. It seems likely therefore that even knot A may not correspond to the core, but may simply correspond to the nearest knot to it, indicating that at this epoch the core is also quenched. The orientation of the knots with respect to the core implies that all three are associated with the same side of the jet (likely to be approaching, although the complex environment of Cygnus X-3 may strongly influence appearances), and were ejected in the sequence C–B–A. Associating knot C with the large radio flare which occurred about a week earlier would imply proper motions in the jet of the order of  $10 \text{ mas d}^{-1}$ , consistent with those reported in Miller-Jones et al. (2004). For a distance of  $\sim 9$  kpc, this corresponds to a projected velocity of  $\sim 0.5c$ , and an intrinsic jet velocity at least as large.

It is interesting to compare the ‘quenching’ of the core radio emission to that observed in the soft X-ray state of black hole candidate X-ray binaries (e.g. Fender et al. 1999b). Gallo, Fender & Pooley (2003) have reported a correlation between X-ray and radio luminosities in black hole candidates in the hard X-ray state, below which the radio emission falls dramatically in softer X-ray states. Assuming a distance of 9 kpc, the core radio emission of Cygnus X-3 in epoch I is almost two orders of magnitude below the correlation, comparable to the strongest limits on quenching found for

other systems. Since neutron stars do not appear to show such strong quenching in soft X-ray states (Migliari et al. 2004 – admittedly this is based on a very small sample), this may be circumstantial evidence that Cygnus X-3 contains a black hole (although the extreme nature of the environment in this system might be responsible in some other way). However, the extreme scattering of X-rays in the system is always going to make it hard to relate the X-ray behaviour to that of the other black hole candidates. It is noteworthy that in many cases ‘residual’ radio emission, such as that we believe we are imaging in epoch I, will limit the extent to which observations on arcsec or coarser angular scales can measure the true extent or rapidity of such quenching. As a result, VLBI observations such as these are required to truly probe rapidly quenched radio states in bright jet sources.

In epoch II, the integrated flux densities from WSRT (1.5 Jy at 5 GHz) and the Ryle Telescope (0.8 Jy at 15 GHz; Fig. 1) reveal a steep spectrum ( $\propto \nu^{-0.6}$ ), indicative of optically thin synchrotron emission. However, since the map presented in Fig. 2 recovers  $\leq 15$  per cent of this integrated flux density, we cannot immediately draw the conclusion that the imaged structures are also therefore optically thin synchrotron emission. Nevertheless, based on simple physical arguments and comparison with other relativistic jet sources, this is likely, and is consistent with the relatively high levels of polarization observed along the jet. As noted above, knot C in particular shows a high level of polarization, which supports the interpretation that it is not the core. The highest fractional polarization, almost 25 per cent, appears to the east of knot B. This is suggestive of an interaction site between the ejected matter and the surrounding medium. The same conjecture can be made about the region of relatively high polarization, 15 per cent, in the north of the complex, albeit with lower confidence due to the fact that artefacts might appear at the edges of the emission. The coincidence of emission at the location of knot C in both epochs may suggest that this is the location of some standing shock in the flow or a site of repeated jet–interstellar medium interactions.

To summarize, a possible explanation for the radio emission detected in the two experiments is the following: the radio-emitting region of epoch I is a jet-like structure probably ejected during the March activity. Epoch II shows multiple radio features of what appears to be a one-sided jet. The new ejecta interact with the material ejected during the previous outburst and generate the high polarization on the eastern edge of the radio structure and a slight bending of the jet in this region towards the south-west [note that precession of the jet is likely to be at work (Mioduszewski et al. 2001; Miller-Jones et al. 2004), thus complicating the interpretation]. The core – corresponding to the location of the X-ray binary, and base of the relativistic jet – is probably not detected at either epoch, indicating a temporary suppression of jet production at these times. It is important to bear in mind that the jet is very close to the line of sight, at an angle of less than  $\sim 15^\circ$  (Mioduszewski et al. 2001; Miller-Jones et al. 2004) – this will cause an exaggeration of apparent bends in the jet, and an underestimate of true jet velocities [see more extensive discussions in Mioduszewski et al. (2001) and Miller-Jones et al. (2004)].

## 4 CONCLUSIONS

We have presented results on the X-ray binary Cygnus X-3 obtained in the framework of the first open call for European e-VLBI observations. The two successful experiments captured Cygnus X-3 initially in an almost quiescent state after the outburst in 2006 March, and subsequently in an active state a few days after the major flare in

2006 May. By the second epoch, a bright, curved, relativistic jet is observed. The total intensity and polarization radio maps provide evidence for interaction of the jet with the surrounding medium and, if our interpretation is correct, with the material ejected in the previous active state. In the first epoch, two weeks prior to the onset of the major flare of 2006 May, the core is in a deeply radio-quenched state, with a  $3\sigma$  upper limit to the flux density of 0.4 mJy. The use of e-VLBI enabled very quick access to the data, practically within one day from the end of the runs, compared with sometimes weeks in the ‘traditional’ VLBI experiments. This facility for rapid response and analysis of VLBI data is of paramount importance for the study of transient sources, enabling decision-making with respect to potential follow-up observations (not only at radio wavelengths) to be much more effective.

#### ACKNOWLEDGMENTS

We thank the JIVE staff R. M. Campbell and C. Reynolds for their valuable contribution to the technical success of the experiments. The European VLBI Network is a joint facility of European, Chinese, South African and other radio astronomy institutes funded by their national research councils. The Ryle Telescope is operated by the University of Cambridge. The X-ray data were provided by the ASM/RXTE teams at MIT and at the RXTE SOF and GOF at NASA’s GSFC. e-VLBI developments in Europe are supported by the EC DG-INFOSO funded Communication Network Development project, ‘EXPREs’, Contract No. 02662.

#### REFERENCES

Becklin E. E., Neugebauer O., Hawkins F., Mason K., Sanford P. W., Matthews K., Wynn-Williams C. G., 1973, *Nat*, 245, 302  
 Choudhury M., Rao A. R., Vadawale S. V., Ishwara-Chandra C. H., Jain A. K., 2002, *A&A*, 383, L35  
 Dhawan V., Mirabel I. F., Rodríguez L. F., 2000, *ApJ*, 543, 373  
 Diamond P. J., 1995, in Zensus J. A., Diamond P. J., Napier P. J., eds, *ASP Conf. Ser. Vol. 82, Very Long Baseline Interferometry and the VLBA*. Astron. Soc. Pac., San Francisco, p. 227  
 Fender R. P., Bell Burnell S. J., Waltman E. B., Pooley G. G., Ghigo F. D., Foster R. S., 1997, *MNRAS*, 288, 849  
 Fender R. P., Hanson M. M., Pooley G. G., 1999a, *MNRAS*, 308, 473  
 Fender R. P. et al., 1999b, *ApJ*, 519, L165  
 Fey A. L. et al., 2004, *AJ*, 127, 3587  
 Gallo E., Fender R. P., Pooley G. G., 2003, *MNRAS*, 344, 60  
 Geldzahler B. J. et al., 1983, *ApJ*, 273, L65  
 Giacconi R., Gorenstein P., Gursky H., Waters J. R., 1967, *ApJ*, 148, L119

Gregory P. C., Kronberg P. P., Seaquist E. R., Hughes V. A., Woodworth A., Viner M. R., Retallack D., 1972, *Nature Phys. Sci.*, 239, 440  
 Koch-Miramond L., Abraham P., Fuchs Y., Bonnet-Bidaud J.-M., Claret A., 2002, *A&A*, 396, 877  
 McCollough M. L. et al., 1999, *ApJ*, 517, 951  
 Martí J., Paredes J. M., Peracaula M., 2001, *A&A*, 375, 476  
 Migliari S., Fender R. P., Rupen M., Wachter S., Jonker P. G., Homan J., van der Klis M., 2004, *MNRAS*, 351, 186  
 Miller-Jones J. C. A., Blundell K. M., Rupen M. P., Mioduszewski A. J., Duffy P., Beasley A. J., 2004, *ApJ*, 600, 368  
 Mioduszewski A. J., Rupen M. P., Hjellming R. M., Pooley G. G., Waltman E. B., 2001, *ApJ*, 553, 766  
 Mitra A., 1998, *ApJ*, 499, 385  
 Molnar L. A., Reid M. J., Grindlay J. E., 1988, *ApJ*, 331, 494  
 Newell S. J., Garrett M. A., Spencer R. E., 1998, *MNRAS*, 293, L17  
 Parsignault D. R. et al., 1972, *Nature Phys. Sci.*, 239, 123  
 Parsley S. et al., 2003, in Minh Y. C., ed., *ASP Conf. Ser. Vol. 306, New technologies in VLBI*. Astron. Soc. Pac., San Francisco, p. 229  
 Pradel N., Charlot P., Lestrade J.-F., 2006, *A&A*, 452, 1099  
 Predehl P., Burwitz V., Paerels F., Trmper J., 2000, *A&A*, 357, L25  
 Rushton A. et al., 2007, *MNRAS*, 374, L11  
 Schalinski C. J. et al., 1995, *ApJ*, 447, 752  
 Schalinski C. J. et al., 1998, *A&A*, 329, 504  
 Schmutz W., Geballe T. R., Schild H., 1996, *A&A*, 311, L25  
 Shepherd M. C., 1997, in Hunt G., Payne H. E., eds, *ASP Conf. Ser. Vol. 125, Astronomical Data Analysis Software and Systems VI*. Astron. Soc. Pac., San Francisco, p. 77  
 Simard-Normandin M., Kronberg P. P., Button S., 1981, *ApJS*, 45, 97  
 Spencer R. E., Swinney R. W., Johnston K. J., Hjellming R. M., 1986, *ApJ*, 309, 694  
 Szomoru A. et al., 2004, in Bachiller R., Colomer F., Desmurs J.-F., de Vicente P., eds, *Proc. 7th Symp. of the European VLBI Network on New Developments in VLBI Science and Technology*. Observatorio Astronómico Nacional, Spain, p. 257  
 van Kerkwijk M. H., Geballe T. R., King D. L., van der Klis M., van Paradijs J., 1996, *A&A*, 314, 521  
 Waltman E. B., Fiedler R. L., Johnston K. L., Ghigo F. D., 1994, *AJ*, 108, 179  
 Waltman E. B., Ghigo F. D., Johnston K. J., Foster R. S., Fiedler R. L., Spencer J. H., 1995, *AJ*, 110, 290  
 Watanabe H., Kitamoto S., Miyamoto S., Fielder R. L., Waltman E. B., Johnston K. J., Ghigo F. D., 1994, *ApJ*, 433, 350  
 Whitney A. R., 2003, in Minh Y. C., ed., *ASP Conf. Ser. Vol. 306, New technologies in VLBI*. Astron. Soc. Pac., San Francisco, p. 123  
 Wilkinson P. N., Narayan R., Spencer R. E., 1994, *MNRAS*, 269, 67

This paper has been typeset from a  $\text{\TeX}/\text{\LaTeX}$  file prepared by the author.